ELSEVIER

www.elsevier.nl/locate/carres

Carbohydrate Research 331 (2001) 393–401

CARBOHYDRATE RESEARCH

# NMR studies of mannitol-terminating oligosaccharides derived by reductive alkaline hydrolysis from brain glycoproteins

Heide Kogelberg*[1], Wengang Chai, Ten Feizi, Alexander M. Lawson*[2]

*The Glycosciences Laboratory, Imperial College School of Medicine, Northwick Park Hospital, Harrow, Middlesex HA1 3UJ, UK*

Received 18 October 2000; received in revised form 9 January 2001; accepted 12 February 2001

**Abstract**

Interest in the characterisation of *O*-mannosyl glycan structures has been stimulated following the identification of mannitol-terminating oligosaccharides among the chains released from mammalian proteins in nervous and muscle tissues, and by the discovery of a putative human *O*-mannosyl transferase. Several mass spectrometry methods have been applied to structure elucidation particularly when low amounts of oligosaccharide are available for analysis. However, when sufficient amounts are available, a combination of through-bond homo- and heteronuclear, and of through-space homonuclear NMR experiments permit the complete identification of these oligosaccharide sequences. We describe here the assignment of $^{1}H$ and $^{13}C$ NMR chemical shifts from such experiments for four mannitol-terminating oligosaccharide alditols, GlcNAcβ-(1→2)Manol, Galβ-(1→4)GlcNAcβ-(1→2)Manol, Galβ-(1→4)[Fucα-(1→3)]GlcNAcβ-(1→2)Manol and NeuAcα-(2→3)Galβ-(1→4)GlcNAcβ-(1→2)Manol, that were released from brain glycopeptides by alkaline borohydride treatment. 

*Keywords:* Brain glycopeptides; $^{1}H$ and $^{13}C$ chemical shifts; Mannitol-terminating oligosaccharides; O-Linked glycans

## 1. Introduction

The important influence of post-translational glycosylation on the properties and functions of proteins is well recognised but remains to be fully elucidated as an increasing diversity of oligosaccharide structures are characterised. Among identified glycans released from glycoproteins by mild alkaline borohydride treatment are a series of glycans terminating in mannose that imply transfer of mannose to Ser/Thr residues in mammalian systems. Previously, mannose was thought to be present as internal residues in *N*-glycans and not present in *O*-glycans of higher eukaryotes, although O-mannosylated proteins occur widely in yeast and fungi. Evidence for

*Abbreviations:* COSY, correlation spectroscopy; DQF-COSY, double quantum filtered-correlated spectroscopy; HMBC, heteronuclear multiple bond correlation; HSQC, heteronuclear single quantum coherence; HSQC-TOCSY, heteronuclear single quantum coherence-total correlation spectroscopy; GalNAcol, *N*-acetylgalactosamminitol; GlcNAcol, *N*-acetylglucosamminitol; Glcol, glucitol; Hex, hexose; HexNAc, *N*-acetylhexosamine; LSIMS, liquid secondary ion mass spectrometry; Manol, mannitol; ROESY, rotating-frame nuclear Overhauser enhancement spectroscopy; TOCSY, total correlation spectroscopy.

[1] * Corresponding author. Tel.: +44-20-88693461; fax: +44-20-88693253; e-mail: h.kogelberg@ic.ac.uk

[2] * Corresponding author. Tel.: +44-20-88693461; fax: +44-20-88693253; e-mail: a.m.lawson@ic.ac.uk

0008-6215/01/$ - see front matter 
PII: S0008-6215(01)00051-9

the presence of *O*-mannosyl glycans was first reported for brain proteoglycans[1–3] and more recently mannose-terminating oligosaccharides carrying an HNK-1 epitope were detected as minor components in total brain glycopeptides.[4] Investigation of the whole pool of structures from this latter source revealed other *O*-mannosyl glycans to be relatively abundant and, in addition, 2-substituted and 2,6-disubstituted mannitol structures were detected for the first time.[5] *O*-mannosyl glycan chains have also been identified on α-dystroglycan from bovine peripheral nerve tissue,[6] rabbit skeletal muscle[7] and sheep brain.[8] A possible role for these glycans in nerve tissue may be to link the extracellular matrix to the cytoskeleton through binding to laminin.[6] Interest in *O*-mannosyl glycan structures on mammalian proteins has been greatly stimulated by the identification of a putative human *O*-mannosyl transferase[9] with homology to functionally significant mannosyl transferases in yeast.

Several approaches have been used for the characterisation of mannose-terminating oligosaccharides as their alditols. Liquid secondary ion mass spectrometry (LSIMS) of permethylated derivatives gives molecular weight information from which monosaccharide composition in terms of dHex, Hex, HexNAc and NeuAc can be deduced, and glycosidic fragmentation that indicates sequence and *N*-acetylhexosamine substitution. Detailed linkage information can be obtained from methylation analysis by GC-MS. A novel approach to sequence determination for the mannitol-terminating oligosaccharides, even when present in complex mixtures, has been the high sensitivity TLC-LSIMS analysis of neoglycolipids derived from the oligosaccharide alditols after treatment with mild periodate oxidation.[4] Methanolysis and LSIMS, and also tandem MS can give oligosaccharide sequence data.[8] Another method has been to label released oligosaccharides with 2-aminobenzamide and monitor the products of selective glycosidase treatment by HPLC with fluorescence detection.[6]

Complete characterisation of oligosaccharide structure can often be carried out by NMR spectroscopy when sufficient amounts are available. For oligosaccharides terminating in *N*-acetylglucosaminitol and *N*-acetylgalactosaminitol there is a wealth of comparative NMR data available (e.g. see http:/www.boc.ruu/nl/sugabase/database.html) to assign N- and O-linked oligosaccharide structures. However, for oligosaccharides terminating in mannitol there has been to our knowledge only one previous report employing NMR, and that was for determining anomeric configurations.[5] Here we describe the comprehensive assignment of $^{1}H$ and $^{13}C$ NMR chemical shifts for four of the mannitol-terminating oligosaccharide alditols obtained from brain glycopeptides. This is important in particular as they corroborate the linkage position of mannitol[4] about which there was disagreement as to whether it was a 2- or 3-linked mannitol, the original assignment being based on minor differences in mass spectra of [$^{2}H_{1}$]-labelled TMS derivatives.[1]

## 2. Experimental

Disaccharide GlcNAcβ-(1→2)Man was purchased from Dextra Laboratories (Reading, UK) and reduced by sodium borohydride to give GlcNAcβ-(1→2)Manol for NMR study. NMR solvent deuterium oxide, $D_2O$ (100.0 atom% D) and $D_2O$ (99.9 atom% D), and internal standard acetone (99.9 + %, HPLC grade) were purchased from Aldrich (Dorset, UK).

*Oligosaccharide alditols isolated from brain glycopeptides.*—Neutral oligosaccharide alditols **2N-1**, **3N-2**, **3N-3** and acidic alditol **3A-5** were isolated from 600 mg non-dialyzable rabbit brain glycopeptides[4] after hydrolysis by alkaline borohydride treatment as described previously.[5] Isolation and purification were carried out by sequential chromatography by gel filtration on Bio-Gel P-4, ion exchange on an Asahipak NH2-P50 column, and HPLC on an APS-2 column. The structures of **2N-1**, **3N-2**, **3N-3** and **3A-5** were previously established as GlcNAcβ-(1→2)Manol, Galβ-(1→4)GlcNAcβ-(1→2)Manol, Galβ-(1→4)[Fucα-(1→3)]GlcNAcβ-(1→2)Manol, NeuAcα-(2→3)Galβ( - 1→4)GlcNAcβ - (1→2)Manol,

respectively, by mass spectrometry with anomeric configurations being defined by NMR.[5]

*Nuclear magnetic resonance spectroscopy.*—NMR spectra were recorded at 15 °C using a Bruker AM400, Varian UNITY plus-500 and Varian UNITY-600. The samples were prepared by repeated dissolution/lyophilization from $D_2O$ and finally dissolved in 500 μL $D_2O$. For heteronuclear NMR experiments Shigemi tubes and 300 μL $D_2O$ were used. Acetone was employed as internal standard ($\delta$ 2.225 ppm for $^1H$ and $\delta$ 31.07 ppm for $^{13}C$ of $CH_3$) and coupling constants were determined on a first-order basis.

1D TOCSY[10,11] spectra of 512 scans were obtained using Gaussian pulses of 90 or 93 ms for anomeric protons and 60 ms for other protons. The duration of the spin-lock period, realised via the MLEV-17[12] sequence, was between 30 and 140 ms. 2D-DQF-COSY spectra were obtained with acquisition times of 76 ms in $t_1$ and 0.3 s in $t_2$ with 32 scans in each $t_1$ increment. Data matrices of $256 \times 1024$ ($t_1 \times t_2$) complex points were acquired, zero-filled to $1024 \times 2048$ ($t_1 \times t_2$) and multiplied prior to Fourier transformation by a Gaussian function. 2D-ROESY[13] spectra were obtained at 400 MHz with a 300 ms spin-lock period. Acquisition times of 51–61 ms and 0.41–0.49 s were used in $t_1$ and $t_2$, respectively. 32 scans were acquired in each of 256 experiments into 2048 complex data points. The 2D matrix was zero-filled to $1024 \times 4098$ ($t_1 \times t_2$) data points and multiplied by a Gaussian function in both dimensions. The spectrum offset was set at the downfield edge of the spectrum in order to minimise TOCSY transfer. 2D gradient-enhanced $^1H/^{13}C$ HSQC[14] spectra were recorded with 15 ms in $t_1$ and 0.15 s in $t_2$, together with 64 scans per $t_1$ increment. $^1H$ decoupling was employed using the GARPI sequence. The data matrix ($t_1$, $t_2$) consisted of $256 \times 384$–$512$ ($t_1 \times t_2$) complex points and was zero-filled to $1024 \times 2048$ ($t_1 \times t_2$) points and multiplied by a Gaussian function prior to Fourier transformation. 2D gradient-enhanced $^1H/^{13}C$ HSQC-TOCSY[15] spectra for **3N-2** and **3N-3** were acquired with 20–42 ms in $t_1$ and 0.15 s in $t_2$, together with 48–96 scans per $t_1$ increment. $^1H$ decoupling was employed using the GARPI sequence. The duration of the spin-lock TOCSY period, realised with the MLEV-17 sequence, was 140 ms. Data matrices of $320$–$512 \times 608$ ($t_1 \times t_2$) complex points were acquired, zero-filled to $1024 \times 2048$ ($t_1 \times t_2$) points and multiplied prior to Fourier transformation by a Gaussian function. The 2D gradient-enhanced HMBC[16] spectrum for **3N-2** was recorded with 15 ms in $t_1$ and 0.293 s in $t_2$, together with 64 scans per $t_1$ increment. The delays were set to 3.4 ms [$1/(2^1J_{CH})$] and 111.1 ms [$1/(2^nJ_{CH})$]. Data matrices of $256 \times 1024$ ($t_1 \times t_2$) complex points were acquired, zero-filled to $1024 \times 2048$ ($t_1 \times t_2$) points and multiplied prior to Fourier transformation by a Gaussian function.

Accurate $^1H$ chemical shift values obtained from 1D spectra are represented to three decimal places and $^1H$ and $^{13}C$ values obtained from 2D spectra to two decimals.

*Mass spectrometry.*—LSIMS was carried out as described[5] on a VG Analytical ZAB2-E mass spectrometer, equipped with a caesium ion gun operated at 25 keV (for negative-ion detection) or 35 keV (for positive-ion detection) with an emission current of 0.5 μA. Acquisition of full scan mass spectra at 20 s/decade was by VG Analytical VAX-Opus data system in continuum acquisition mode. Negative ion mode was employed for native oligosaccharide alditols and positive ion for permethylated derivatives. Typically, ~1 μg of sample was used for analysis with thioglycerol as the liquid matrix.

## 3. Results and discussion

Chemical shifts and sequence assignments for the oligosaccharide alditols **2N-1**, **3N-2**, **3N-3** and **3A-5** were made from through-bond homonuclear (DQF-COSY, 1D TOCSY) and heteronuclear (HSQC, HSQC-TOCSY, HMBC) NMR spectra, and from through-space homonuclear (2D ROESY) spectra.

*Disaccharide **2N-1**: GlcNAcβ-(1→2)-Manol.*—The disaccharide **2N-1** was isolated from brain glycopeptides that gave a LSIMS $[M-H]^-$ ion at $m/z$ 384 from which its composition was deduced to be Hex.HexNAc in reduced form. The sequence of **2N-1** was

identified as HexNAc-Hexol from the spectrum of its permethylated derivative (Fig. 1) from the glycosidic cleavage ion at $m/z$ 260 indicating a non-reducing terminal HexNAc. Methylation analysis identified the alditol as Manol and that it was substituted at C-2 by a GlcNAc.[5] As only a small amount of **2N-1** was isolated and its $^1$H NMR spectrum found to be identical to the spectrum of the reduced synthetic disaccharide GlcNAcβ-(1→2)Manol (data not shown), the synthetic material was then used to carry out the complete NMR assignment. This disaccharide gives single anomeric $^1$H and $^{13}$C NMR chemical shifts at $\delta = 4.700$ and 101.93 ppm, respectively (Tables 1 and 2). The complete spin system of the GlcNAc residue can be assigned from COSY and TOCSY spectra with the coupling constant $^3J_{\text{H-1,H-2}} = 8.4$ Hz identifying a β configuration.[5] The reduced Manol residue can be identified from two spin systems, H-1, H-1′, H-2, H-3 and H-4, H-5, H-6, H-6′, because of the small coupling constant between H-3 and H-4. The linkage of GlcNAc to the C-2 of Manol is apparent from $^{13}$C chemical shift differences for C-1, C-2 and C-3 of Manol ($-2.67$, 8.07 and $-2.04$ ppm, respectively) in comparison with unsubstituted Manol.[17] $^1$H chemical shift differences are also observed for H-2, H-3 and H-4 of Manol in **2N-1** (0.12, 0.15 and 0.12 ppm, respectively) when compared to unsubstituted Manol.[18] In addition, the linkage is corroborated from a ROESY spectrum by an interglycosidic connectivity between GlcNAc H-1 and Manol H-2 (Table 3), and a weaker connectivity between GlcNAc H-1 and Manol H-3.

*Trisaccharide **3N-2**: Galβ-(1→4)GlcNAcβ-(1→2)Manol.*—$^1$H and $^{13}$C chemical shifts of the reducing end GlcNAcβ-(1→2)Manol of the trisaccharide are similar to those of the disaccharide **2N-1** (Tables 1 and 2). The Gal residue can be assigned from the characteristic spin system connecting H-1 to H-4, as the coupling constant between H-4 and H-5 is small. Gal is in β configuration with a vicinal coupling constant of 7.9 Hz between H-1 and H-2.[5] The linkage of Gal to C-4 of GlcNAc is apparent from the $^{13}$C chemical shift differences of C-3, C-4 and C-5 of GlcNAc ($-1.32$, 8.45 and $-1.02$ ppm, respectively) when compared to those in **2N-1**. Comparative $^1$H chemical shift differences for H-3, H-4 and H-5 (0.179, 0.291 and 0.140 ppm, respectively) are also observed. Two strong inter-glycosidic connectivities are present in the 2D ROESY spectrum of **3N-2** (Table 3), one between GlcNAc H-1 and Manol H-2 and another between Gal H-1 and GlcNAc H-4, and a weak connectivity is observed between GlcNAc H-1 and Manol H-3. When long range inter-glycosidic connectivities are traced by through-bond H,C couplings in a HMBC spectrum, the GlcNAcβ-(1→2)Manol and the Galβ-(1→4)GlcNAc linkages can be confirmed (Table 3).

*Tetrasaccharide **3N-3**: Galβ-(1→4)[Fucα-(1→3)]GlcNAcβ-(1→2)Manol.*—The Galβ-(1→4)GlcNAcβ-(1→2)Manol sequence of **3N-3** can be assigned as described for **3N-2**, with similar $^1$H and $^{13}$C chemical shifts (Tables 1 and 2). The $^{13}$C chemical shift differences for C-3 and C-4 of GlcNAc (2.35 and $-5.02$ ppm, respectively) when compared

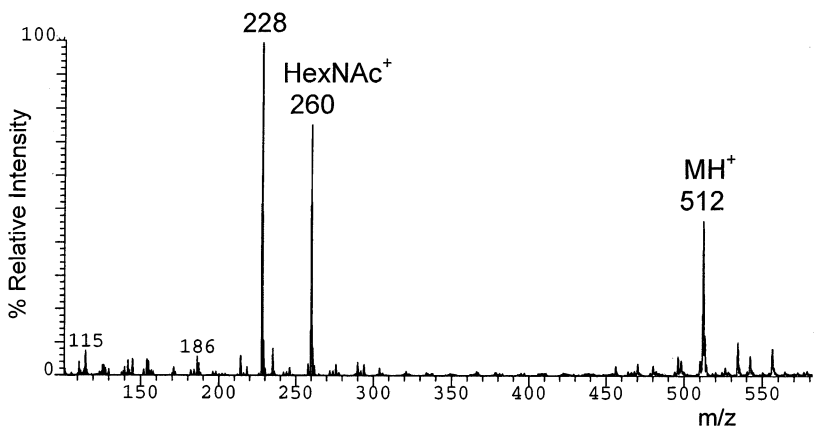


Fig. 1. LSIMS spectrum of oligosaccharide **2N-1** as its permethylated derivative.

Table 1
$^1$H chemical shifts ($\delta$, ppm) and coupling constants ($^3J_{H,H}$, Hz) of oligosaccharides **2N-1**, **3N-2**, **3N-3** and **3A-5** [a]

| Compound | Residue | H-1/H-1′ | H-2 | H-3 | H-4 | H-5 | H-6/H-6′ | | NAc |
|---|---|---|---|---|---|---|---|---|---|
| **2N-1** | Manol, $\delta$ | 3.868 [b]/3.744 | 3.868 [b] | 3.936 | 3.905 | 3.741 | 3.856/3.656 | | |
| | $\Delta\delta_{(2N-1)-(Manol)}$ | 0.008/0.074 | 0.12 | 0.15 | 0.12 | −0.009 | −0.004, −0.014 | | |
| | $^3J_{H,H}$ | $6.4_{1',2}$, $-11.5_{1,1'}$ | [c] | $<1.0_{3,4}$ | $9.1_{4,5}$ | $2.7_{5,6}$ | $6.4_{5,6'}$, $-11.7_{6,6'}$ | | |
| | GlcNAc, $\delta$ | 4.700 | 3.714 | 3.562 | 3.45 | 3.46 | 3.929/3.746 | | 2.049 |
| | $^3J_{H,H}$ | $8.4_{1,2}$ | $10.4_{2,3}$ | $8.1_{3,4}$ | [c] | [c] | $5.3_{5,6'}$, $-12.3_{6,6'}$ | | |
| **3N-2** | Manol, $\delta$ | 3.871 [b]/3.75 | 3.871 [b] | 3.939 | 3.901 | 3.735 | 3.856/3.657 | | |
| | $^3J_{H,H}$ | [c] | $8.0_{2,3}$ | $1.1_{3,4}$ | $9.0_{4,5}$ | $2.7_{5,6}$ | $6.4_{5,6'}$, $-11.7_{6,6'}$ | | |
| | GlcNAc, $\delta$ | 4.721 | 3.76 | 3.741 [b] | 3.741 [b] | 3.601 | 3.991/3.832 | | 2.046 |
| | $\Delta\delta_{(3N-2)-(2N-1)}$ | 0.021 | 0.046 | 0.179 | 0.291 | 0.140 | 0.062/0.086 | | |
| | $^3J_{H,H}$ | $7.9_{1,2}$ | [c] | [c] | [c] | $2.2_{5,6}$ | $5.5_{5,6'}$, $-12.1_{6,6'}$ | | |
| | Gal, $\delta$ | 4.461 | 3.532 | 3.664 | 3.918 | 3.72 | 3.741 [b]/3.741 [b] | | |
| | $^3J_{H,H}$ | $7.9_{1,2}$ | $9.9_{2,3}$ | $3.3_{3,4}$ | [c] | [c] | [c] | | |
| **3N-3** | Manol, $\delta$ | 3.86/3.75 | 3.87 | 3.94 | 3.91 | 3.74 | 3.85/3.67 | | |
| | GlcNAc, $\delta$ | 4.730 | 3.91 | 3.90 | 3.93 | 3.598 | 4.004/3.856 | | 2.037 |
| | $\Delta\delta_{(3N-3)-(3N-2)}$ | 0.009 | 0.15 | 0.159 | 0.189 | −0.003 | 0.013/0.024 | | |
| | $^3J_{H,H}$ | $7.8_{1,2}$ | [c] | [c] | [c] | $2.1_{5,6}$ | $-12.3_{6,6'}$ | | |
| | Gal, $\delta$ | 4.440 | 3.495 | 3.655 | 3.893 | 3.60 | 3.72/3.72 | | |
| | $^3J_{H,H}$ | $7.8_{1,2}$ | $10.1_{2,3}$ | n.d. [d] | ~1.0 | [c] | [c] | | |
| | Fuc, $\delta$ | 5.119 | 3.688 | 3.907 | 3.792 | 4.850 | 1.174 | | |
| | $^3J_{H,H}$ | $4.0_{1,2}$ | n.d. | $2.6_{3,4}$ | $<1.0_{4,5}$ | $6.6_{5,6}$ | | | |
| **3A-5** | Manol, $\delta$ | 3.86/3.73 | 3.88 | 3.940 | 3.895 | 3.73 | 3.85/3.66 | | |
| | $^3J_{H,H}$ | [c] | [c] | [c] | $9.0_{4,5}$ | n.d. | n.d. | | |
| | GlcNAc, $\delta$ | 4.714 | 3.739 [b] | 3.739 [b] | 3.739 [b] | 3.602 | 4.002/3.851 | | 2.043 |
| | $^3J_{H,H}$ | $7.9_{1,2}$ | [c] | [c] | [c] | $2.0_{5,6}$, | $-12.3_{6,6'}$ | | |
| | Gal, $\delta$ | 4.544 | 3.564 | 4.117 | 3.979 | 3.739 [b] | 3.739 [b]/3.739 [b] | | |
| | $\Delta\delta_{(3A-5)-(3N-2)}$ | 0.083 | 0.032 | 0.453 | 0.061 | 0.019 | −0.002/−0.002 | | |
| | $^3J_{H,H}$ | $7.9_{1,2}$ | $9.9_{2,3}$ | $3.1_{3,4}$ | [c] | [c] | [c] | | |
| | | H-3ax/H-3eq | H-4 | H-5 | H-6 | H-7 | H-8 | H-9/H-9′ | NAc |
| | NeuAc, $\delta$ | 1.801/2.713 | 3.677 | 3.854 | 3.625 | 3.60 | 3.90 | 3.87/3.64 | 2.029 |
| | $^3J_{H,H}$ | $-12.5_{3ax,3eq}$, $4.5_{3eq,4}$ | $12.3_{3ax,4}$ | n.d. | n.d. | n.d. | n.d. | n.d. | |

[a] $^1$H chemical shifts differences ($\Delta\delta$) are indicated between the reducing end mannitol of **2N-1** and of Manol, between the GlcNAc residue of **3N-2** and of **2N-1**, between the GlcNAc residue of **3N-3** and of **3N-2**, and between the Gal residue of **3A-5** and of **2N-1**.

[b] The middle point of the multiplet higher order is indicated.

[c] Signals of higher order.

[d] n.d., not determined.

with **3N-2** identifies the C-3 of GlcNAc as the linkage site for the additional monosaccharide. Downfield $^1$H chemical shifts for GlcNAc are observed for H-2, H-3 and H-4 (0.15, 0.159 and 0.189 ppm, respectively) when compared with those in **3N-2**. As for **2N-1**, the two separate spin systems (H-1, H-1′, H-2, H-3 and H-4, H-5, H-6, H-6′) that aid the assignment of Manol are observed in this case in a $^1$H, $^{13}$C HSQC-TOCSY spectrum (data not shown). The Fuc monosaccharide is readily identified from structural reporter groups,[19] the anomeric $^1$H chemical shift at 5.119 ppm and the methyl group at 1.174 ppm, in addi-

Table 2
$^{13}$C chemical shifts ($\delta$, ppm) of oligosaccharides **2N-1**, **3N-2**, **3N-3** and **3A-5** [a]

| Compound | Residue | C-1 | C-2 | C-3 | C-4 | C-5 | C-6 | | NAc |
|---|---|---|---|---|---|---|---|---|---|
| **2N-1** | Manol, $\delta$ | 61.93 | 80.27 | 68.66 | 69.86 | 71.58 | 64.15 | | |
| | $\Delta\delta_{(2N-1)-(Manol)}$ | −2.67 | 8.07 | −2.04 | −0.84 | −0.62 | −0.45 | | |
| | GlcNAc, $\delta$ | 101.93 | 56.63 | 74.72 | 70.81 | 76.59 | 61.59 | | 23.02 |
| **3N-2** | Manol, $\delta$ | 61.92 | 80.32 | 68.70 | 69.88 | 71.58 | 64.16 | | |
| | GlcNAc, $\delta$ | 101.84 | 56.21 | 73.40 | 79.26 | 75.57 | 60.92 | | 23.04 |
| | $\Delta\delta_{(3N-2)-(2N-1)}$ | −0.09 | −0.42 | −1.32 | 8.45 | −1.02 | 0.33 | | |
| | Gal, $\delta$ | 103.83 | 71.89 | 73.40 | 69.47 | 76.29 | 61.96 | | |
| **3N-3** | Manol, $\delta$ | 61.88 | 80.35 | 68.65 | 69.97 | 71.48 | 64.11 | | |
| | GlcNAc, $\delta$ | 101.60 | 56.93 | 75.75 | 74.24 | 75.93 | 60.68 | | 23.13 |
| | $\Delta\delta_{(3N-3)-(3N-2)}$ | −0.24 | 0.72 | 2.35 | −5.02 | 0.36 | −0.24 | | |
| | Gal, $\delta$ | 102.79 | 71.92 | 73.29 | 69.24 | 75.93 | 62.46 | | |
| | Fuc, $\delta$ | 99.60 | 68.59 | 69.97 | 72.78 | 67.63 | 16.31 | | |
| **3A-5** | Manol, $\delta$ | 61.92 | 80.27 | 68.71 | 69.91 | 71.63 | 64.14 | | |
| | GlcNAc, $\delta$ | 101.86 | 56.19 | 73.36 | 79.13 | 75.60 | 60.86 | | 23.08 |
| | Gal, $\delta$ | 103.52 | 70.35 | 76.38 | 68.37 | 76.06 | 61.92 | | |
| | $\Delta\delta_{(3A-5)-(3N-2)}$ | −0.31 | −1.54 | 2.98 | −1.1 | −0.23 | −0.04 | | |
| | | C-3 | C-4 | C-5 | C-6 | C-7 | C-8 | C-9 | NAc |
| | NeuAc, $\delta$ | 40.52 | 69.37 | 52.56 | 73.86 | 69.00 | 72.76 | 63.46 | 22.88 |

[a] $^{13}$C chemical shift differences ($\Delta\delta$) are indicated between the reducing end Manol of **2N-1** and of Manol, between the GlcNAc residue of **3N-2** and of **2N-1**, between the GlcNAc residue of **3N-3** and of **3N-2**, and between the Gal residue of **3A-5** and of **2N-1**.

tion to the $^{13}$C chemical shifts of C-1 at 99.60 ppm and the methyl carbon at 16.31 ppm. $^{1}$H and $^{13}$C chemical shift differences of GlcNAc when compared to **3N-2** (see above), an interglycosidic ROE between Fuc H-1 and GlcNAc H-3 (Fig. 3 and Table 3) and the vicinal $^{1}$H,$^{1}$H coupling constant between H-1 and H-2 of 4.0 Hz,[5] identify the Fuc$\alpha$-(1→3)GlcNAc linkage. **3N-3** contains the classical Le$^{x}$ epitope, which manifests itself by a large downfield $^{1}$H chemical shift of Fuc H-5 at 4.850 ppm (Table 1) and remote ROE connectivities between Fuc H-5 and Gal H-2, and between Fuc H-6 and Gal H-2 (Fig. 2 and Table 3) as a result of Fuc-Gal stacking interactions.[20]

*Tetrasaccharide **3A-5**: NeuAc$\alpha$-(2→3)Gal$\beta$-(1→4)GlcNAc$\beta$-(1→2)Manol.*—The Gal$\beta$-(1→4)GlcNAc$\beta$-(1→2)Manol sequence of **3A-5** is identified as in **3N-2** with the addition of a $^{1}$H,$^{13}$C HSQC-TOCSY spectrum to assign Manol (data not shown). Major $^{13}$C chemical shift differences are observed for C-2, C-3 and C-4 of Gal of **3A-5** (−1.54, 2.98 and −1.1 ppm, respectively, Table 2) when compared to those of **3N-2**, thus identifying C-3 as the linkage site for Gal. This can also be deduced from the $^{1}$H downfield chemical shift of 0.453 ppm for H-3 of Gal when compared with **3N-3**. As expected for a NeuAc-Gal linkage, the neighbouring protons Gal H-2 and Gal H-4 are not affected by glycosylation. The NeuAc residue is readily identified from the

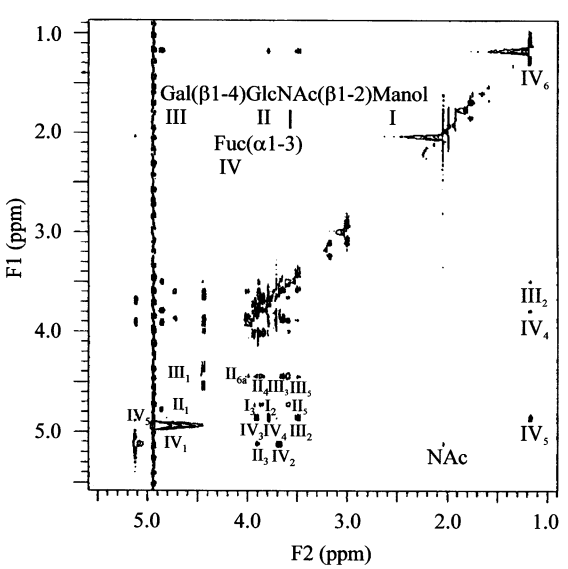


Fig. 2. 2D ROESY spectrum of tetrasaccharide, **3N-3**. Intra- and intermolecular rOe connectivities are indicated.

Table 3
Interglycosidic correlations of oligosaccharides **2N-1**, **3N-2**, **3N-3** and **3A-5**

| Compound | Anomeric $^1$H | ROE to | HMBC to | Correlations |
|---|---|---|---|---|
| **2N-1** | | | | |
| GlcNAc-(β1-2)Manol | 4.700, $II_1$ | 3.868, $I_2$ [a] | | $II_1$–$I_2$ |
| II I | | 3.936, $I_3$ [b] | | |
| | | 3.562, $II_3$ | | |
| | | 3.454, $II_5$ | | |
| **3N-2** | | | | |
| Gal-(β1-4)GlcNAc-(β1-2)Manol | 4.721, $II_1$ | 3.87, $I_2$ [a] | 80.32, $I_2$ | $II_1$-$I_2$ |
| III II I | | 3.94, $I_3$ [b] | 73.40, $II_3$ | |
| | | 3.60, $II_5$ | | |
| | | 3.74, $II_3$ | | |
| | 4.461, $III_1$ | 3.74, $III_5$,$II_4$ | 79.26, $II_4$ | $III_1$-$II_4$ |
| | | 3.66, $III_3$ | 71.89, $III_2$ | |
| | | | 73.40, $III_3$ | |
| **3N-3** | | | | |
| Gal-(β1-4)GlcNAc-(β1-2)Manol | 4.73, $II_1$ | 3.87, $I_2$ [a] | | $II_1$-$I_2$ |
| III II \| I | | 3.94, $I_3$ [b] | | |
| Fuc(α1-3) | | 3.60, $II_5$ | | |
| IV | 4.44, $III_1$ | 3.93, $II_4$ | | $III_1$-$II_4$ |
| | | 3.86, $II_{6b}$ | | |
| | | 3.66, $III_3$ | | |
| | | 3.60, $III_5$ | | |
| | 5.12, $IV_1$ | 3.90, $II_3$ | | $IV_1$-$II_3$ |
| | | 3.69, $IV_2$ | | |
| | | 2.04, $II_{NAc}$ | | |
| | Others | | | |
| | 4.85, $IV_5$ | 3.50, $III_2$ | | |
| | | 3.90, $IV_3$ | | |
| | | 3.79, $IV_4$ | | |
| | | 1.17, $IV_6$ | | |
| | 1.17, $IV_6$ | 3.50, $III_2$ | | |
| | | 3.79, $IV_4$ | | |
| | | 4.85, $IV_5$ | | |
| **3A-5** | | | | |
| NeuAc-(α2-3)Gal-(β1-4)GlcNAc-(β1-2)Manol | 4.71, $II_1$ | 3.88, $I_2$ [a] | | $II_1$-$I_2$ |
| IV III II I | | 3.94, $I_3$ [b] | | |
| | | 3.74, $II_3$ | | |
| | | 3.60, $II_5$ | | |
| | 4.54, $III_1$ | 3.74, $II_4$,$III_5$ | | $III_1$-$II_4$ |
| | | 4.12, $III_3$ | | |
| | Others | | | |
| | 1.80, $IV_{3ax}$ | 4.12, $III_3$ | | $IV_2$-$III_3$ |
| | | 3.85, $IV_5$ | | |
| | | 2.71, $IV_{3eq}$ | | |

[a] strong; [b] weak

structural reporter groups, H-3ax and H-3eq (1.801 and 2.713 ppm, respectively) with C-3 at 40.52 ppm (Fig. 3 and Tables 1 and 2). The $^1$H spin system of NeuAc is traced from H-3ax to H-6 by through-bond correlations using TOCSY spectra with increased mixing times (data not shown). $^1$H and $^{13}$C chemical shifts of positions 5 and 6 of NeuAc are identified from characteristic carbon shifts in the HSQC spectrum (Fig. 3), while those at positions 7 and 8 can be assigned based on the reported values for NeuAcα-(2→3)Galβ-(1→4)-GlcNAc.[21] The NeuAcα-(2→3)Gal linkage is assigned from an interglycosidic ROE connectivity between NeuAc H-3ax and Gal H-3 (Table 3).

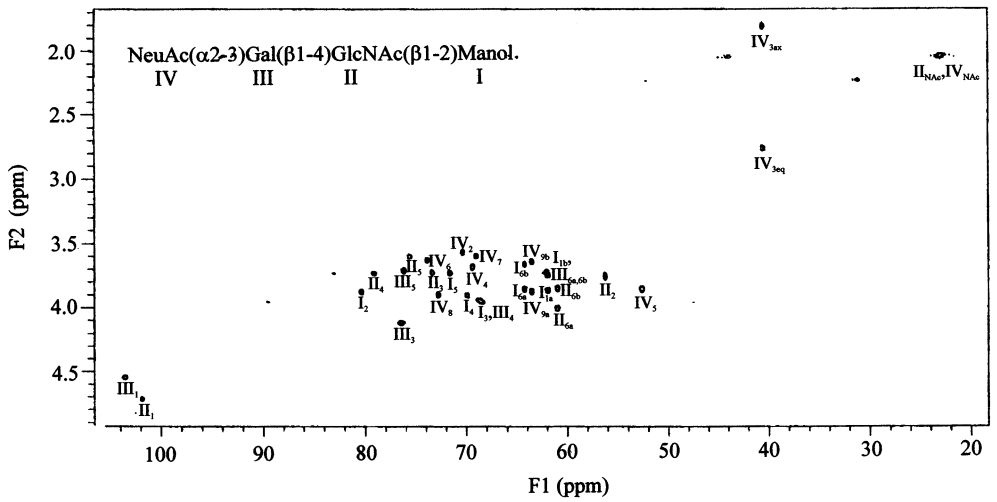


Fig. 3. 2D HSQC spectrum of tetrasaccharide, **3A-5**. Cross peak assignments are indicated.

## 4. Conclusions

In summary, the $^{1}H$ and $^{13}C$ NMR chemical shifts have been assigned for a series of mannitol-terminating oligosaccharides released from brain glycopeptides by alkaline borohydride treatment. The mannitol residue does not contain a structural reporter group in the proton dimension. However, two methylene carbon atoms can be readily identified, of which C-1 is shifted to higher field than C-6, thus assigning C-2 as the linkage position. The non-reducing terminal sequences linked to the mannitol that are described, GlcNAcβ-(1→, Galβ-(1→4GlcNAcβ-(1→, Galβ-(1→4)[Fucα-(1→3)]-GlcNAcβ-(1→ and NeuAcα-(2→3)Galβ-(1→4)GlcNAcβ-(1→, are common to *O*-GalNAc-linked glycoproteins. In mucin-like proteins, *O*-GalNAc glycosylation has a pronounced effect on the conformation of the protein core, significantly extending chain dimensions and decreasing the flexibility of the chain,[22] and the importance of the methyl group of the core GalNAc residue has been suggested.[23] It will be of interest to extend the present study of free oligosaccharide alditols and to investigate in glycopeptides the influence of the core mannose linkage on the amino acid backbone as has been studied in *O*-GalNAc-containing mucins.[22] Different three-dimensional presentation can be envisaged for oligosaccharide chains when linked to *O*-GalNAc or *O*-mannosyl which might well be translated into different biological activities.

## Acknowledgements

This work was supported by a Medical Research Council (MRC) programme grant (G9601454). NMR experiments were performed at the MRC Biomedical NMR Centre, London. We are grateful to Drs M.J. Gradwell and T.A. Frenkiel for help with heteronuclear NMR experiments.

## References

[1] Finne, J.; Krusius, T.; Margolis, R. K.; Margolis, R. U. *J. Biol. Chem.* **1979**, *254*, 10295–10300.
[2] Krusius, T.; Finne, J.; Margolis, R. K.; Margolis, R. U. *J. Biol. Chem.* **1986**, *261*, 8237–8242.
[3] Krusius, T.; Reinhold, V. N.; Margolis, R. K.; Margolis, R. U. *Biochem. J.* **1987**, *245*, 229–234.
[4] Yuen, C.-T.; Chai, W.; Loveless, R. W.; Lawson, A. M.; Margolis, R. U.; Feizi, T. *J. Biol. Chem.* **1997**, *272*, 8924–8931.
[5] Chai, W.; Yuen, C.-T.; Kogelberg, H.; Carruthers, R. A.; Margolis, R. U.; Feizi, T.; Lawson, A. M. *Eur. J. Biochem.* **1999**, *263*, 879–888.
[6] Chiba, A.; Matsumura, K.; Yamada, H.; Inazu, T.; Shimizu, T.; Kusunoki, S.; Kanazawa, I.; Kobata, A.; Endo, T. *J. Biol. Chem.* **1997**, *272*, 2156–2162.
[7] Sasaki, T.; Yamada, H.; Matsumura, K.; Shimizu, T.; Kobata, A.; Endo, T. *Biochim. Biophys. Acta* **1998**, *1425*, 599–606.
[8] Smalheiser, N. R.; Haslam, S. M.; Sutton-Smith, M.; Morris, H. R.; Dell, A. *J. Biol. Chem.* **1998**, *273*, 23698–23703.
[9] Jurado, L. A. P.; Coloma, A.; Cruces, J. *Genomics* **1999**, *58*, 171–180.
[10] Kessler, H.; Anders, V.; Gemecker, B.; Steuernagel, S. *J. Magn. Reson.* **1989**, *85*, 1–14.
[11] Gradwell, M. J.; Kogelberg, H.; Frenkiel, T. A. *J. Magn. Reson.* **1997**, *124*, 267–270.

[12] Bax, A.; Davies, D. G. *J. Magn. Reson.* **1985**, *65*, 355–360.
[13] Bax, A.; Davies, D. G. *J. Magn. Reson.* **1985**, *63*, 207–213.
[14] Wider, E.; Wüthrich, K. *J. Magn. Reson.* **1993**, *102*, 239–241.
[15] Lerner, L. E.; Bax, A. *J. Magn. Reson.* **1986**, *69*, 375–380.
[16] Parella, T.; Sanchez-Ferrando, F.; Virgili, A. *J. Magn. Reson.* **1995**, *117*, 78–83.
[17] Angyal, S. J.; LeFur, R. *Carbohydr. Res.* **1980**, *84*, 201–209.
[18] Hawkes G. E., Lewis D., *J. Chem. Soc. Perkin. Trans. II*, **1984**, 2073–2078.
[19] Vliegenthart, J. F.; Dorland, L.; van Halbeek, H. *Carbohydr. Chem. Biochem.* **1983**, *41*, 209–374.
[20] Ichikawa, Y.; Lin, Y.-C.; Dumas, D. P.; Shen, G.-S.; Garcia-Junceda, E.; Williams, M. A.; Bayer, R.; Ketcham, C.; Paulson, J. C.; Wong, C.-H. *J. Am. Chem. Soc.* **1992**, *114*, 9283–9298.
[21] Breg, J.; Kroon-Batenburg, L. M.; Strecker, G.; Montreuil, J.; Vliegenthart, J. F. *Eur. J. Biochem.* **1989**, *178*, 727–739.
[22] Gerken, T. A.; Butenhof, K. J.; Shogren, R. *Biochemistry* **1989**, *28*, 5536–5543.
[23] Live, D. H.; Williams, L. J.; Kuduk, S. D.; Schwarz, J. B.; Glunz, P. W.; Chen, X. T.; Sames, D.; Kumar, R. A.; Danishefsky, S. J. *Proc. Natl. Acad. Sci. USA* **1999**, *96*, 3489–3493.